

# Centre to limb darkening of stars

## New model and application to stellar interferometry

**D. Hestroffer**

Astrophysics Division, ESTEC, Postbus 299, 2200 AG Noordwijk, The Netherlands (e-mail: dhestrof@estec.esa.nl)

Received 19 February 1997 / Accepted 13 June 1997

**Abstract.** Measurement of a star's apparent diameter with an intensity interferometer yields its geometrical radius and its effective temperature when one knows or measures the specific centre to limb-darkening. This paper presents a formulation that (1) makes use of a single parameter and (2) is well suited for the interpretation and comparison of centre to limb darkening. Subsequently, this result is applied to the study of the contrast of the fringes as obtained with a stellar interferometer. A method yielding the angular diameter of the extended source together with the parameter of the law modeling its centre to limb darkening is presented. The value of such observations made by GAIA type interferometer (Lindegren & Perryman 1996) are briefly noted in the last section.

**Key words:** limb darkening – stars: fundamental parameters of – stars: atmospheres of – GAIA – techniques: interferometric.

---

### 1. Introduction

The angular diameter is an important parameter for stellar evolution studies. When combined with the parallax it yields the linear radius of a star, and also a model-free measurement of its effective temperature. Evolution of interferometric techniques in the past decades has shown the potential of such observations to retrieve these fundamental parameters. They are less restricted in sky coverage than the lunar occultation technique; in the optical domain, they remain however limited to bright objects. Knowledge of the centre to limb darkening, i.e. the variation of the specific intensity across the stellar disc, is important in the derivation of the angular diameter from observed fluxes or from interferometric methods. It also plays an important role in the analysis of eclipsing binary light curves or lunar occultation observations. The centre to limb darkening is expressed as the specific intensity versus  $\mu = \cos \theta$ , the cosine of the azimuth of a surface element of the star, and normalised for

$\mu = 1$ . The most frequently adopted empirical law is given by a polynomial function:

$$I_{\lambda}^*(\mu)/I_{\lambda}^*(1) = 1 - \sum_{i \geq 1} a_i (1 - \mu)^i \quad (1)$$

where  $I_{\lambda}^*(\mu)$  is the brightness of a point source at wavelength  $\lambda$ ,  $I_{\lambda}^*(1)$  is the brightness at the centre and  $a_i = a_i(\lambda)$  are limb darkening coefficients for given band-pass. We will only consider in this paper the normalised brightness that we write for brevity  $I_{\lambda}(\mu)$ . In the Eddington approximation the limb darkening is:

$$I_{\lambda}(\mu) = 1 - \frac{3}{5} (1 - \mu)$$

Usually, when the linear model fails, the brightness distribution is modeled by the quadratic law:

$$I_{\lambda}(\mu) = 1 - a_1 (1 - \mu) - a_2 (1 - \mu)^2 \quad (2)$$

except for the Sun where the approximation has to be given at least by a five degree polynomial (e.g. Pierce & Slaughter 1977; Neckel & Labs 1994). Other laws were also introduced during the last decades (e.g. Klingsmith & Sobieski 1970; Cheng et al. 1986; Rubashevskii 1991; Díaz-Cordovés & Giménez 1992; Díaz-Cordovés et al. 1995):

$$I_{\lambda}(\mu) = \begin{cases} 1 - a_1 (1 - \mu) - a_2 (1 - \mu)^p \\ 1 - a_1 (1 - \mu) - a_2 \mu \ln \mu \\ 1 - a_1 (1 - \mu) - a_2 (1 - \sqrt{\mu}) \\ 1 - a_1 \left( 1 - \cos \left( \frac{\pi}{2} \sqrt{1 - \mu^2} \right) \right) \end{cases}$$

For a discussion and comparison of some of these laws see Van Hamme (1993) and Díaz-Cordovés et al. (1995). It turns out that towards longer wavelength and in the IR the 'square root' law is more appropriate; in the UV the 'logarithmic law' yields a better approximation; and in the optical region, better results are obtained with the logarithmic law for cool stars and with the square root law for higher temperatures. For general purposes, the coefficients are derived from the calculated brightness distribution – obtained from extensive grids of different stellar atmospheres models – by least-squares fits (e.g. Manduca et al. 1977; Claret & Giménez 1990;

Van Hamme 1993), adding on occasion a condition on the conservation of integrated fluxes. However each law has some limitations and the coefficients have never been determined from observations. Thus the radii, effective temperatures and angular diameters derived from interferometric observations are model dependent.

We now introduce another empirical model that is well adapted to express the observed solar limb darkening, but also matches well the computed functions for static and Mira M giant models as derived by Scholz & Takeda (1987). This model is intended to yield an approximation of the calculated brightness distribution at least as good as a quadratic model but with less parameters. It is useful for modeling binary stars light curves, lunar occultation of stars, or the observations of resolved stars by interferometric techniques (speckle, stellar interferometer). It is also intended to yield an analytical formulation for the simultaneous determination of the angular diameter of a star together with its brightness distribution from interferometric observations.

In the following Section I present the law and the comparison with observed or other calculated brightness distributions. In the subsequent section, the corresponding analytical formulation of the visibility function for an intensity interferometer is given. Following it is shown under what circumstances one can derive un-biased values of the apparent diameter and the centre to limb darkening function. I briefly expose in the last sections what can be expected in this domain with ground-based observations or by an interferometer like GAIA.

## 2. Power law for limb darkening

In the following  $x$ ,  $\mu$  and  $\alpha$  are real numbers such that:  $x \geq 0$ ,  $0 \leq \mu \leq 1$  and  $\alpha \geq 0$ . We introduce another empirical brightness distribution function:

$$I_\lambda(\mu) = \mu^\alpha \quad ; \quad \alpha \in \mathbb{R}^+ \quad (3)$$

This one parameter power law can be seen as a particular case of the law of Minnaert (1961) for a reflecting body seen at full phase ( $I(\mu, \mu_o) = \mu_o^k \mu^{k-1}$  when  $\mu_o = \mu$ ), that is when the cosines of the azimuth of the emissive and receptive points are equal. Any brightness distribution of this kind yields a fully darkened disc (i.e.  $I(\mu = 0) = 0$ ) for  $\alpha > 0$ . Fig. 1 shows the centre to limb darkening of Eq. (3) versus  $\mu$  and  $r$ . We find here the particular cases of uniform brightness for  $\alpha = 0$ , and (linear) fully darkened disc for  $\alpha = 1$ .

### 2.1. Radius of a star

The cosine  $\mu$  used in the previous sections is related to a given layer of the star, and hence to a given radius. The definition of the radius is important since the observations correspond to the photosphere which may be larger than the radius of the model especially for giants. On an observational point of view one refers to the outermost layer (Baschek et al. 1991). Let  $r_\lambda$  be the wavelength dependent (monochromatic or filter integrated) intensity-radius of the outermost layer, and  $R$  the optical-depth Rosseland

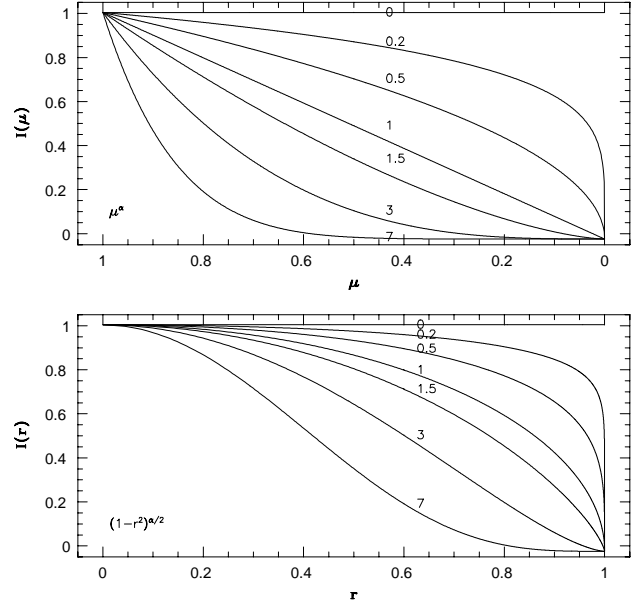


**Fig. 1.** Centre to limb darkening derived from the power law in Eq. (3); as a function of  $\mu$  (top), and versus the distance from the star centre  $r$ , in units of the photosphere radius (bottom). The different curves correspond to different values of the exponent  $\alpha$

radius  $R = r(\bar{\tau}_{\text{Ross}} = 1)$ . Introducing the photospheric extension  $d_\lambda = r_\lambda/R - 1$ , we have the relation on the cosines  $\mu_R$  and  $\mu_{r_\lambda}$  corresponding respectively to the radii  $R$  and  $r_\lambda$ :

$$\mu_R = [1 - (1 - \mu_{r_\lambda}^2)(1 + d_\lambda)^2]^{1/2}$$

Here the value of the radius  $r_\lambda$  is such that – within the precision of the measured quantity –  $I_\lambda(r = r_\lambda) = I_\lambda(\mu_{r_\lambda} = 0) \approx 0$ . For a compact atmosphere, we have  $\mu_R = \mu_{r_\lambda} = \mu$  referring to any layer independently of the wavelength. For extended atmospheres however, the relation between the different radii is more troublesome (Baschek et al. 1991; Scholz 1997).

### 2.2. Comparison to observed and calculated values

As noted previously, the single parameter power law in Eq. (3) yields at the limb:  $I(\mu = 0) = 0$ ,  $\forall \alpha > 0$ . If the disc is not fully darkened, one may introduce the two-parameters law:

$$I_\lambda(\mu) = 1 - u(1 - \mu^\alpha) \quad (4)$$

This yield a good fit, as shown in Fig. 2 with  $u = 0.86$  and  $\alpha = 0.68$ , to the observed limb darkening of the Sun when  $\mu \geq 0.02$  (Allen 1973). This comparison is limited to a typical wavelength only, and shows the value of such an approximation. It is stressed that the five-degree polynomial derived by Neckel & Labs (1994) was not fitted to the same set of observations and was limited to data at more than  $7''$  from the limb in order to avoid seeing effects.

On the other hand, static M-giants stellar models predict a fully darkened disc with more or less pronounced intensity gradients (Scholz & Takeda 1987). Fig. 3 gives, for a relatively

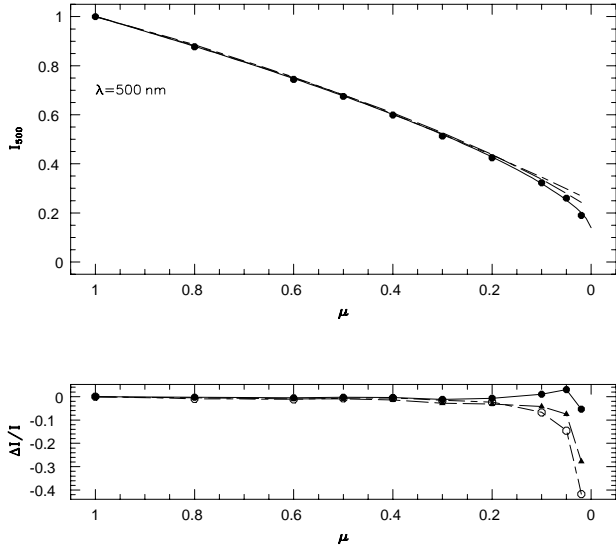


**Fig. 2.** Observed and empirical solar limb darkening at 500 nm (top), and corresponding residuals (bottom). In the upper panel, filled circles correspond to the observations as compiled by Allen (1973), the solid line corresponds to the power law model and dashed lines to (linear and quadratic) polynomial models. In the lower panel, open circles correspond to the quadratic model of Allen (1973), filled triangles correspond to an interpolation of the 5 degrees polynomial of Neckel & Labs (1994), and filled circles to the power law. The latter is best suited for near-limb observations, and it yields a standard deviation on the normalised difference of 0.02

compact star, a comparison of a quadratic and power law fit when the photospheric extension is known. The model surface  $r_o = r(\bar{\tau}_{\text{Ross}} = 10^{-5})$  used for static M-giants models by Scholz & Takeda (1987) is chosen with respect to the largest intensity radius  $r_\lambda$  of the strongest absorption features for these almost compact stars with steep gradient  $\partial I / \partial \mu$ . The linear distance  $\delta$  related to the stellar atmosphere model is given in Scholz and Takeda's paper by  $0 \leq \delta \leq r_o / R = 1 + d$ . In this case, the power law, with a single parameter, represents the brightness distribution at least as well as a quadratic fit. For Miras stars, in contrast to the power law, the quadratic fit is inappropriate (Scholz & Takeda 1987). A more detailed analysis should be made by computing parameters and residuals for brightness distributions of various stellar models, which is not in the scope of this study.

### 2.3. Summary

In terms of quality of the fit to observed or calculated values of axially symmetric brightness distribution, the power law introduced here is able to reproduce the values well, and needs only one parameter. Such a law also exhibits the steeper  $\partial I / \partial \mu$  gradients at the limb as well as the pronounced wings in  $I(r)$  although the actual behaviour at the limb is neither easy to observe nor to predict (see discussion in Scholz & Takeda 1987). For general purposes the power law is a good approximation, though for particular wavelengths, effective temperatures, etc.,

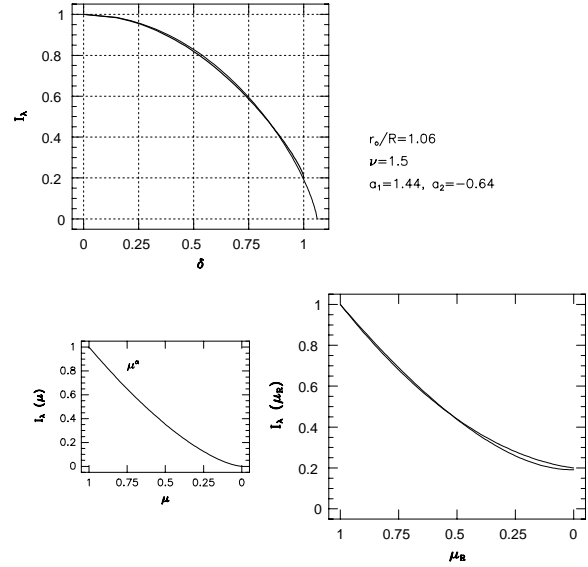


**Fig. 3.** Empirical quadratic and power law. The parameters are derived from a fit to a brightness distribution corresponding to a static model  $T_{eff} / \log g / [A/H] = 3500 / 1.3 / 0$ ,  $d = 6\%$ , with a filter  $\lambda = 400$  nm,  $\Delta\lambda = 5$  nm compiled by Scholz & Takeda (1987)

other laws may be more appropriate in terms of the residuals. Based on the theoretical centre to limb variation and on the previous remarks, we will adopt in the following sections the center to limb variation parameterization given by Eq. (3).

## 3. Visibility function

While it is more natural to deal with the power  $\alpha$  for the brightness distribution itself, we introduce, for the study of the visibility function arising in observations by interferometric techniques, the more appropriate quantity  $\nu = \alpha / 2 + 1$  which will be used in the rest of this paper.

### 3.1. Derivation from power law parameterization

When observing a resolved object with a stellar interferometer, the contrast or visibility of the fringes diminish with increasing baseline length. For a radially symmetric brightness distribution across a disc, the visibility function at any spatial frequency can be obtained from the Hankel transform<sup>1</sup>:

$$V = \frac{\left| \int_0^\infty I(r) J_0(xr) r dr \right|}{\int_0^\infty I(r) r dr} \quad (5)$$

where the spatial frequency is:

$$x = \frac{\pi \phi B}{\lambda}$$

<sup>1</sup> As we suppose that both the brightness distribution and the shape are radially symmetric, only the amplitude visibility is of interest, while the phase and imaginary part are null.

$B$  is the separation of the pupils,  $\lambda$  is the effective wavelength and  $\phi$  is the apparent diameter (corresponding to the true zero-intensity radius). Under these assumptions and taking a brightness distribution following Eq. (3), the visibility function becomes:

$$V_\nu(x) = 2\nu \left| \int_0^1 (1-r^2)^{\nu-1} J_0(xr) r dr \right|$$

yielding:

$$\begin{aligned} V_\nu(x) &= \Gamma(\nu+1) \frac{|J_\nu(x)|}{(x/2)^\nu} \\ &= |{}_0F_1(\nu+1; -x^2/4)| \end{aligned} \quad (6)$$

where  $J_\nu$  is the Bessel function of first kind, and  ${}_0F_1$  is the generalized hypergeometric function. The visibility function is similar – with an appropriate scaling of the spatial frequency – to the ‘modulation function’ of a resolved object observed with a modulating grid (Hestroffer & Mignard 1997). This function is shown in Fig. 4 for different exponents  $\nu$ . For a sharp gradient

$$\frac{\partial I_\lambda(0)}{\partial \mu} \rightarrow \infty$$

the fringes disappear at the zeros of Bessel function; on the other hand for very weak gradients

$$\frac{\partial^p I_\lambda(0)}{\partial \mu^p} = 0, \quad p \geq 1$$

which correspond to  $\nu \gg 1$ , the visibility vanishes for high values of the spatial frequency (see Fig. 4).

Introducing the continuously differentiable function:

$$\tilde{V}_\nu(x) = {}_0F_1(\nu+1; -x^2/4) \quad \text{and} \quad \varepsilon_x = \text{sgn}(\tilde{V}_\nu(x)) \quad (7)$$

we have  $V_\nu = \varepsilon_x \tilde{V}_\nu$ , and for any real value  $\nu$ , the power expansion:

$$\tilde{V}_\nu(x) = \sum_{k \geq 0} \frac{1}{k! (\nu+1)_k} (-x^2/4)^k \quad (8)$$

where  $(\nu+1)_k \equiv \Gamma(\nu+1+k)/\Gamma(\nu+1)$  is the Pochhammer symbol.

### 3.2. Approximations

Given the diameter of the equivalent uniform disc  $\phi_{\text{ud}}$  as derived from a fit to the visibility function (under the a priori hypothesis of a uniform brightness distribution), and the limb darkening parameter  $\nu$  (observed or calculated), one can derive an approximation of a more realistic limb darkened diameter as often found in the literature. We find, when  $\nu$  is not too large, the scaling factor:

$$\phi_\nu / \phi_{\text{ud}} \sim 1 + 2(\nu-1)(x_{3/2}/x_1 - 1) \quad ; \quad \nu \lesssim 2$$

where  $x_{3/2} \simeq 4.49$  and  $x_1 \simeq 3.83$  are the zeros of the Bessel functions  $J_{3/2}$  and  $J_1$ . The previous approximation is best suited for observations spread around the first zero of the visibility function. One will however prefer to determine directly the model-free diameter.

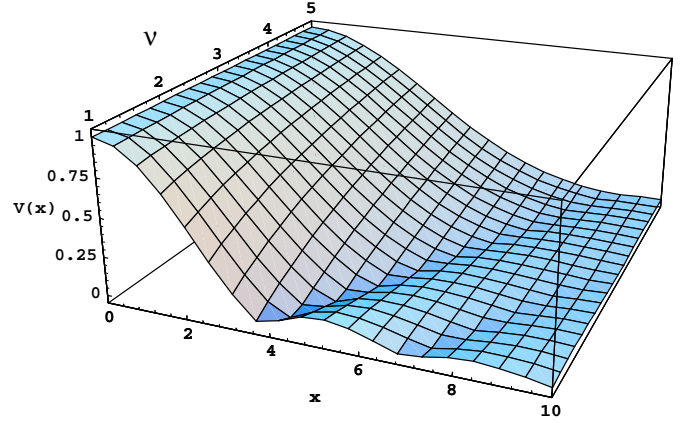


**Fig. 4.** Visibility function  $V(x)$  versus spatial frequency  $x$  and as a function of the exponent  $\nu$ , which is also related to the brightness gradient

If we take Lommel’s expansion of Eq. (7) as a series of Bessel functions ( $\tau \neq \nu$ ):

$$\tilde{V}_\nu(x) = \frac{\Gamma(\nu+1)\Gamma(\tau+1)}{\Gamma(\nu-\tau)} \sum_{k \geq 0} \frac{\Gamma(\nu-\tau+k)}{k! \Gamma(\nu+k+1)} \frac{J_{\tau+k}(x)}{(x/2)^{\tau-k}}$$

putting respectively  $\tau = 1$  and  $\tau = 3/2$ , we can write the weighted mean:

$$\tilde{V}_\nu(x) = \left( \frac{a}{2} + \frac{b}{3} \right)^{-1} \times \left[ \frac{a}{2} \tilde{V}_1(x) + \frac{b}{3} \tilde{V}_{3/2}(x) + \sum_{k \geq 1} R_k(x) \right] \quad (9)$$

where  $\sum_{k \geq 1} R_k$  is the rest. With  $a = 1 - u$ ,  $b = u$  we find, in the first terms, the visibility function  $V_{\text{lin}}(x)$  derived by Hanbury Brown et al. (1974) for the linear model  $I(\mu) = 1 - u(1 - \mu)$ . Thus brightness distributions differing even significantly at the limb can yield similar visibility amplitudes over a large interval of spatial frequency (see Fig. 5).

### 3.3. Gaussian fit

Some observed visibility functions in the visible wave-bands are better represented by a ‘Gaussian fit’ (e.g. Wilson et al. 1992; Tuthill et al. 1994; Haniff et al. 1995), especially when the contrast does not vanish as expected for a uniformly bright disc. One can note however that this also appears for a power law distribution with  $\nu \gtrsim 5$  (see Fig. 4). In particular, the Gaussian fit can also be seen as a special case of a more general power law fit with  $\nu \approx 8.3$  since both parameterization yield similar visibility functions. Moreover, it is stressed that models involving asymmetric distributions (e.g. spots) can also yield such a feature for the visibility function (e.g. Di Benedetto & Bonneau 1990; Wilson et al. 1992).

## 4. Determination of limb-darkening and radius

### 4.1. Determination from observations

For a given wavelength, it is not possible to infer the brightness distribution and the angular diameter from observations

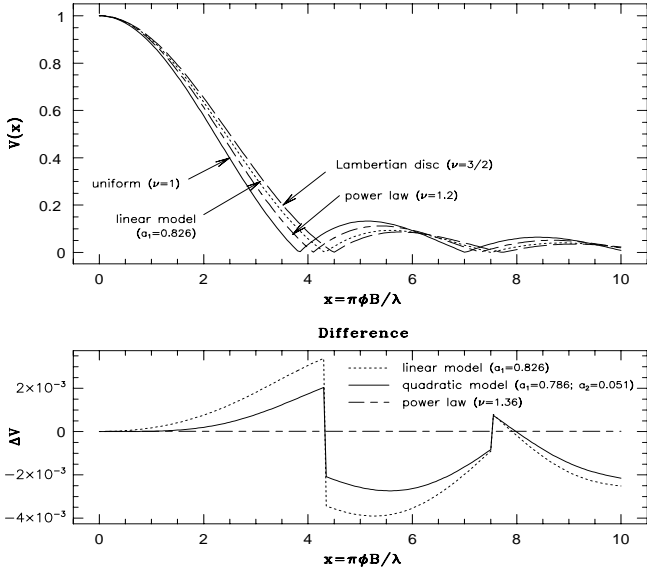


**Fig. 5.** Visibility function for different centre to limb darkening models (top). Difference between a linear, a quadratic and a power law model (bottom). The parameters of the linear and quadratic fits are taken from Manduca et al. (1977) for a star with stellar model  $T_{\text{eff}}/\log g/[A/H] = 6000/3.0/0$

gathered around a single spatial frequency (in particular in the vicinity of the first zero of the visibility function). Then for each adopted brightness distribution, one finds a corresponding model-dependent angular diameter. On the other hand, if it is possible to derive a parameterization of the centre-to-limb variation that fits the visibility of the fringes, one can derive the intensity radius of the star. This inverse problem has never been formulated, and we should see under what conditions and with what precision one can determine simultaneously both parameters. Such estimations can be done with the analytical formulation given in the previous sections.

Let  $\phi_o$  be the angular diameter obtained from the spatial frequency corresponding to the first zero of the contrast (or more generally to a measured contrast) and for an uniformly bright disc  $\nu_o = 1$  (or close to the true value). The true diameter and limb-darkening coefficient will slightly deviate from these initial values, so that we may determine these by a linearised least-squares solution. The discrepancy between the measured visibility function and the calculated one:

$$\Delta V = V_{\text{obs}}(x) - {}_0F_1(\nu_o + 1; -x^2/4) \quad (10)$$

can arise from an error in the brightness-model parameter and an error in the apparent diameter  $\phi_o$ . The major problem is the separability of the unknowns because a small change in either the apparent diameter or the limb darkening parameter yields similar visibility functions (see Fig. 6).

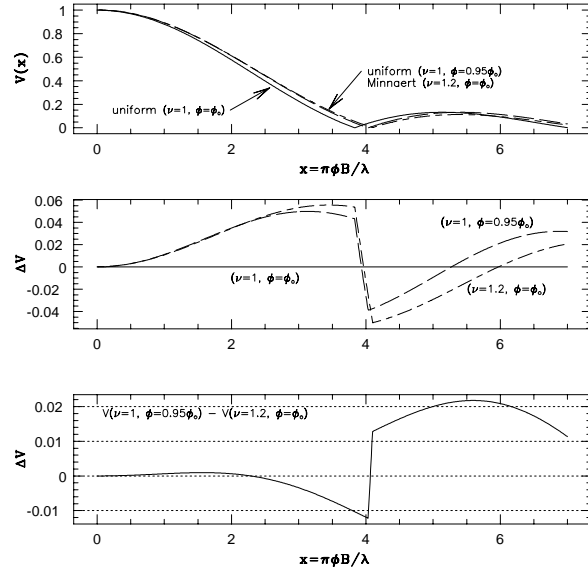


**Fig. 6.** Influence on the visibility function of small changes in brightness distribution and apparent diameter. Upper panel: visibility functions for a uniformly bright star and for slightly different parameters. Middle panel: residuals with respect to  $V_1(\phi_o)$ . Lower panel: residuals  $V_1(0.95\phi) - V_{1.2}(\phi)$

#### 4.1.1. A change in the diameter

Noting that  $d\phi/\phi = dx/x$ , this may be considered as a variation  $d\phi/\phi$ :

$$V_\nu(\phi_o + d\phi/\phi) = V_\nu(\phi_o) + x \frac{\partial V_\nu}{\partial x} d\phi/\phi + o(d\phi)^2$$

Expressing this with the continuously differentiable function  $\tilde{V}_\nu(x)$  defined in Eq. (7), we find the partial derivative:

$$\begin{aligned} \frac{\partial \tilde{V}_\nu(x)}{\partial x} &= -\frac{x}{2(\nu+1)} {}_0F_1(\nu+2; -x^2/4) \\ &= -\frac{x}{2(\nu+1)} \tilde{V}_{\nu+1}(x) \end{aligned}$$

hence

$$x \frac{\partial \tilde{V}_\nu(x)}{\partial x} = -\frac{x^2}{2(\nu+1)} \tilde{V}_{\nu+1}(x)$$

which yields for  $\nu_o = 1$ :

$$x \frac{\partial \tilde{V}_1(x)}{\partial x} = -2 J_2(x) \quad (11)$$

#### 4.1.2. A change in the power law parameter

A deviation from the brightness distribution parameter is expressed by:

$$V_{\nu_o+d\nu}(x) = V_{\nu_o}(x) + \frac{\partial V_{\nu_o}(x)}{\partial \nu} d\nu + o(d\nu)^2$$

Derivation of the Pochhammer symbol yields:

$$\frac{\partial}{\partial \nu} \left\{ \frac{1}{(\nu+1)_k} \right\} = -\frac{1}{(\nu+1)_k} [\psi(\nu+1+k) - \psi(\nu+1)]$$

where  $\psi(z) = \frac{\Gamma'(z)}{\Gamma(z)}$  is the digamma function, hence we have the differential equation:

$$\psi(\nu) {}_0F_1(\nu; z) - \frac{\partial}{\partial \nu} {}_0F_1(\nu; z) = \sum_{k \geq 0} \frac{\psi(\nu+k)}{k! (\nu)_k} z^k$$

thus from Eq. (8):

$$\frac{\partial \tilde{V}_\nu(x)}{\partial \nu} = \psi(\nu+1) \tilde{V}_\nu(x) - \sum_{k \geq 0} \frac{\psi(\nu+1+k)}{k! (\nu+1)_k} (-x^2/4)^k \quad (12)$$

which yield for  $\nu_o = 1$ :

$$\frac{\partial \tilde{V}_1(x)}{\partial \nu} = (1/2 - \gamma) \tilde{V}_1(x) - \sum_{k \geq 0} \frac{\psi(k+2)}{(k+1)(k!)^2} (-x^2/4)^k \quad (13)$$

where  $\gamma$  is Euler's constant.

#### 4.2. Least-squares solution

The equations of condition of the linearised problem are:

$$dV = \varepsilon_x d\tilde{V} = \varepsilon_x \left( x \frac{\partial V_{\nu_o}(x_o)}{\partial x} \quad \frac{\partial V_{\nu_o}(x_o)}{\partial \nu} \right) \cdot \begin{pmatrix} d\phi/\phi \\ d\nu \end{pmatrix}$$

The sign  $\varepsilon_x$  is of no importance here, and we write in matrix form:

$$\Delta \tilde{V} = \mathbf{A} \begin{pmatrix} d\phi/\phi \\ d\nu \end{pmatrix} \quad (14)$$

When the normal matrix is not singular one obtains the solution:

$$\begin{pmatrix} d\phi/\phi \\ d\nu \end{pmatrix} = (\mathbf{A}'\mathbf{A})^{-1} \mathbf{A}' \Delta V$$

and the variance matrix for the unknowns  $(\mathbf{A}'\mathbf{A})^{-1}$ .

It is interesting, from this analytical formulation, to see whether the partial derivatives are close to zero for particular values of  $x$ , in which cases the observations are well suited for un-biased determination of a single parameter. We can also obtain an estimation of the accuracy for the simultaneous determination of the unknowns. As a first approach we will only consider the case  $\nu_o = 1$ , although the same procedure can be applied when  $\nu_o \gg 1$ . The graphs of these partial derivatives are given in Fig. 7.

One can note that both derivatives vanish for different values of spatial frequency. Thus (1) observations around  $x \sim 5$  are less sensitive to an error in the diameter and (2) observations in the vicinity of  $x \sim 6$  are less sensitive to an error in the brightness distribution.

For an observation in the visible domain at  $\lambda = 500$  nm, one finds the corresponding length of the baseline:

$$B \phi = \frac{x\lambda}{\pi} \sim \begin{cases} 164 \\ 197 \end{cases} \quad B \text{ in metres and } \phi \text{ in mas}$$

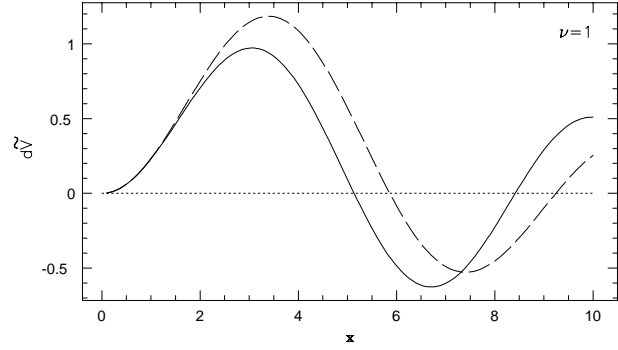


**Fig. 7.** Partial derivatives of the function  $\tilde{V}_1$ . Solid curve:  $-\frac{\partial \tilde{V}_1(x)}{\partial x}$ ; dashed curve:  $4 \frac{\partial \tilde{V}_1(x)}{\partial \nu}$

This corresponds for an object of diameter  $\phi = 10$  mas to 16.4 and 19.7 m respectively. For observations in the IR domain the values are larger. These baselines are not achievable by the 4 m GHRIL (Ground-Based High Resolution Imaging Laboratory at the William Herschel Telescope), but they are for instance well suited to the 31.5 m MkIII optical interferometer located on Mt. Wilson, the 67 m GI2T (Grand Interferomètre à 2 Télescopes, Calern observatory) and in the near-infrared, the 38 m IOTA (Infrared Optical Telescope Array, Mt. Hopkins).

If one has  $N$  well-calibrated observations of a single star regularly spread over the spatial frequency range  $0 < x \leq x_m$ , one can evaluate from Eq. (14) the precisions  $\sigma_\phi$  and  $\sigma_\nu$  of the unknown parameters as a function of the number of observations and the precision of the measure  $\sigma_o = \sigma_{\Delta V}$ . The hypothesis of uniformly distributed observations is of course not constraining and invoked only for convenience of calculation. We can write the following formula for the estimation of the standard deviation:

$$\begin{aligned} \sigma_\phi &= \xi \sigma_o \\ \sigma_\nu &= 4 \eta \sigma_o \end{aligned} \quad (15)$$

so that  $\xi$  and  $\eta$  are characteristic of the accuracy of the solution. The smaller are these two coefficients, the higher is the precision of the determination of the apparent diameter and the limb-darkening parameter. Hence one will prefer a sufficiently large number of measures of the visibility with a high precision for  $\sigma_o$ , but also an optimal distribution of these observations over the spatial frequency domain to enable a determination of the two parameters  $\phi$  and  $\nu$  with a good precision.

If there exists a linear combination such that, for all  $x$ ,

$$a \frac{\partial V(x)}{\partial x} + b \frac{\partial V(x)}{\partial \nu} \sim 0;$$

the Jacobian matrix  $\mathbf{A}$  would be ill-conditioned leading to large values for  $\xi$  and  $\eta$ , and the derived corrections are unrealistic. It reflects the fact that, whatever the number of observations and the precision of a single visibility measurement, it is not possible to separate the unknowns. We see from Fig. 7, that for  $x \lesssim 2$  the observations only provide the single linear combination  $d\nu - 4d\phi/\phi = 0$ , thus either  $\nu$  or  $\phi$  has to be determined by

**Table 1.** Characteristic degree of accuracy for the simultaneous determination of apparent diameter and limb darkening parameter

$x_m$	3	4	5	6	7	$x_o$
$\xi$	8.51	3.01	1.46	0.93	0.80	0.54
$\eta$	7.76	2.55	1.14	0.73	0.66	0.45
$\rho$	$3 \cdot 10^3$	$5 \cdot 10^2$	$1 \cdot 10^2$	36.4	25.2	2.9

other means. This is however not always the case, hence we can in theory determine both unknowns with an accuracy increasing with number of non redundant observations.

Taking a constant number of observations, one finds five variance matrices corresponding to  $x_m = 3, 4, 5, 6, 7$ . The results are shown in Table 1 for  $N = 29$  observations. The last line gives the condition number  $\rho$  of the normal matrix. A high condition number reflects the inability to separate the two unknowns, while when  $\rho = 1$ , the unknowns are un-correlated. The last column (labeled  $x_o$ ) is given for comparison when  $4.5 < x \leq 6.5$  and with the same number of observations.

It can be seen from the decreasing characteristic coefficients  $\xi$  and  $\nu$  in Table 1 that, for the same number of observations, each of precision  $\sigma_o$ , the angular diameter and the limb-darkening parameter  $\alpha = \nu - 1/2$  are better determined when measurements are extended to large spatial frequencies. One also sees that, while observations made at small spatial frequency are unable to yield a unique solution, those made on the second lobe of the visibility function are of high value. In between, care must be taken on the preconditioning of the problem. Indeed the relatively high condition number for  $x_m = 7$  is essentially a consequence of the predominant and degrading observations with  $x \lesssim 3$ . A better result, although not optimal, is obtained by considering only the subset of observations in the range  $4.5 < x \leq 6.5$  as seen in Table 1, the correlation in this case is 0.46.

As an application of these results ( $\nu_o = 1$ ), for the best conditioned system (column  $x_o$ ), observations distributed with a step  $\Delta x = 1/15$ , and a realistic precision for a normal point  $\sigma_o = 0.02$ , one finds from Eq. (15):

$$\sigma_\phi = 1\% \quad \text{and} \quad \sigma_\nu \simeq 0.04$$

yielding an un-biased determination of the angular diameter with a good precision.

#### 4.3. Discussion

We have seen in the previous sections that one can derive the apparent diameter together with a parameterization of the brightness distribution from observations with a long-baseline stellar interferometer. This is possible when a precision of about 0.02 in the measure of the visibility is achieved and the observations are performed at least up to the ‘first zero’ (i.e.  $x \approx 4$ ). We have also shown that care must be taken on the preconditioning of the system of normal equations when one wishes to determine these parameters from an arbitrary set of observations. When the simultaneous determination of the parameters  $\phi$  and  $\nu$  is not possible, more realistic model-dependent angular diameters

can also be derived by tabulating the parameter  $\nu$  from a stellar atmosphere model. The power-law model may fit various observed visibility functions, although it nevertheless assumes radially symmetric brightness distribution across the stellar disc. It can be extended to the case of elongated disc and image reconstruction, but did not consider the case of stars with small scale structure like spots. We have implicitly considered the intensity radius; the relation to any other radius (e.g. optical depth radius) for extended atmospheres, or for very diffuse limb (i.e. weak intensity gradients) is more troublesome and not under the scope of the present study. Simultaneous determination of the apparent diameter and brightness-distribution parameterization enters in the scope of ground-based observation campaigns or space missions.

### 5. Observations with GAIA

GAIA (Global Astrometric Interferometer for Astrophysics) is a preliminary concept for an astrometric mission within the context of ESA’s ‘Horizon 2000 Plus’ programme (Lindegren & Perryman 1996). In its present form, observations are carried out in the spectral range  $350 \leq \lambda \leq 800$  nm with a limiting magnitude  $V < 15$  mag, which also allows observations of a few hundreds of asteroids (Hestroffer & Morando 1995). The experiment is estimated to lead to parallaxes and proper motions of tens of millions of objects accurate to  $10 - 20 \mu\text{as}$ . As a by-product it should therefore yield angular diameters of hundreds of celestial bodies (nearby, giant stars and asteroids) down to  $\phi \approx 5$  mas, and detect partially resolved objects down to  $\phi \approx 2$  mas (Hestroffer & Vakili, in prep.). It should thus provide effective temperatures to compare for instance with those obtained by the infrared flux method (Blackwell & Shallis 1977). Alternatively, when separate determination of both brightness distribution and apparent diameter is not possible, such observations will however provide, for a fixed diameter, the variation of the limb darkening coefficient with wavelength, showing the behaviour of the atmosphere in the near-continuum. With a nominal mission duration of 5 years and different position angles of the interferometer baseline, it will be possible to detect multiple and double stars, and also particular features on stellar atmospheres yielding high-resolution images such as those obtained from ground for Betelgeuse and Mira by Wilson et al. (1992). Similarly it will be possible to detect eventual long-term diameter variations as observed by Tuthill et al. (1995) or Quirrenbach et al. (1994). Also GAIA will enable the investigation of the pulsation properties and qualify current dynamical models (Tuthill et al. 1994; Haniff et al. 1995; Gillet et al. 1990).

### 6. Conclusion

The power law should be a good approximation to the centre to limb brightness variation, especially for reduction of observations obtained by interferometric techniques. It reproduces qualitatively the limb darkening of compact stars or of very extended photospheres. The simplest power law assumes that the

brightness distribution is radially symmetric, and that the intensity drops to zero at the outermost layer of the atmosphere. We have derived an analytical formulation of the visibility function arising in interferometric observations. It has been shown under what circumstances observations with long-baseline interferometers can yield simultaneously an un-biased estimation of the angular diameter and the limb-darkening parameter of the power-law parameterization. This particular study is not exhaustive and should be enlarged to very pronounced limb darkening. With a 2.45 m baseline, the optical space interferometer GAIA should yield at least the equivalent diameters  $\phi_{\text{UD}}$  for more than hundred stars, and hence high precision linear radii and effective temperatures.

*Acknowledgements.* The author is grateful to P. Charlot, F. Vakili and D. Bonneau for their valuable comments. Thanks also go to M.A.C. Perryman for reading the manuscript. The author is indebted to the referee M. Scholz, for his critical remarks and constructive review of this paper. The author acknowledges receipt of a research fellowship from the European Space Agency.

## References

- Allen C.W., 1973, *Astrophysical Quantities*, 3rd edition, Athlone Press, London
- Baschek B., Scholz M., Wehrse R., 1991, *A&A* 246, 374
- Blackwell D.E., Shallis M.J., 1977, *MNRAS* 180, 177
- Cheng A.Y.S., Hege E.K., Hubbard E.N., et al., 1986, *ApJ* 309, 737
- Claret A., Giménez A., 1990, *A&A* 230, 412
- Di Benedetto G.P., Bonneau D., 1990, *ApJ* 358, 617
- Díaz-Cordovés J., Giménez A., 1992, *A&A* 259, 227
- Díaz-Cordovés J., Claret A., Giménez A., 1995, *A&A* 259, 227
- Gillet D., Burki G., Duquenois A., 1990, *A&A* 237, 159
- Hanbury-Brown R., Davis J., Lake R.J.W., Thompson R.J., 1974, *MNRAS* 167, 475
- Haniff C.A., Scholz M., Tuthill P.G., 1995, *MNRAS* 276, 640
- Hestroffer D., Mignard F., 1997, *A&A* (in press)
- Hestroffer D., Morando B., 1995, In: *Future possibilities for astrometry in space. Joint RGO-ESA workshop*, Cambridge, UK, 19-21 June 1995. ESA SP-379, 41
- Klinglesmith D.A., Sobieski S., 1970, *AJ* 75, 175
- Lindgren L., Perryman M.A.C., 1996, *A&AS* 116, 579
- Manduca A., Bell R.A., Gustafsson B., 1977, *A&A* 61, 809
- Minnaert M., 1961, In: *Planets and Satellites*, vol 3, The Solar System. Kuiper, Middlehurst (eds.), p. 213
- Neckel H., Labs D., 1994, *Solar Physics* 153, 91
- Pierce A.K., Slaughter C.D., 1977, *Solar Physics* 51, 25
- Quirrenbach A., Mozurkewich D., Hummel C.A., Armstrong J.T., 1994, *A&A* 285, 541
- Rubashevskii A.A., 1991, *SvA* 35, 626
- Scholz M., 1997, In: *Fundamental Stellar Properties: The interaction between observation and theory*. Bedding T.R., Booth A.J., Davis J. (eds). IAU Symp. 189, Kluwer, Dordrecht (in press)
- Scholz M., Takeda Y., 1987, *A&A* 186, 200. *Erratum* *A&A* 196, 342
- Tuthill P.G., Haniff C.A., Baldwin J.E., Feast M.W., 1994, *MNRAS* 266, 745
- Tuthill P.G., Haniff C.A., Baldwin J.E., 1995, *MNRAS* 277, 1541
- Van Hamme W., 1993, *AJ* 106, 2097
- Wilson R.W., Baldwin J.E., Busher D.F., Warner P.J., 1992, *MNRAS* 257, 369